*Kovove Mater. 51 2013 117–122*
*DOI: 10.4149/km_2013_2_117*


# Thermal stability of the ultrafine grained EN AW 6082 aluminium alloy

M. Fujda[1]*, M. Matvija[1], T. Kvačkaj[2], O. Milkovič[1], P. Zubko[1], K. Nagyová[1], P. Sláma[3]

[1] *Technical University of Košice, Faculty of Metallurgy, Department of Materials Science, Park Komenského 11, 040 01 Košice, Slovak Republic*
[2] *Technical University of Košice, Faculty of Metallurgy, Department of Metals Forming, Vysokoškolská 4, 040 01 Košice, Slovak Republic*
[3] *COMTES FHT, a. s., Průmyslová 995, 334 41 Dobřany, Czech Republic*

Received 13 January 2012, received in revised form 27 September 2012, accepted 2 October 2012

**Abstract**

The initially annealed EN AW 6082 aluminium alloy was processed by ECAP-technique (equal-channel angular pressing) at room temperature following route $B_C$ up to 6 passes. Equiaxed ultrafine subgrains (main subgrain size of 370 nm) with a high dislocation density were formed by the severe plastic deformation of the fine grained initially annealed alloy state (main grain size of 6.7 μm). The result of the observed refinement and strain hardening of the solid solution was an increase in tensile strength and, on the other hand, a decrease in tensile ductility of the analysed alloy.

The formed ultrafine grained microstructure and mechanical properties of ECAPed alloy state was relatively stable up to post-ECAP annealing temperature of 200 °C. The continuous recrystallization of the solid solution and its uniform grain growth was a result of the post--ECAP annealing at temperatures up to 275 °C. Even though the strength of the severely deformed alloy was considerably reduced by this annealing treatment, its yield strength ($R_{p0.2}$) was almost twice that of the fully recrystallized initially annealed alloy state. Annealing at the highest temperature of 350 °C initiated a non-uniform solid solution grain growth and a formation of the bimodal grain size distribution. This discontinuously recrystallized alloy state exhibited the typical strain hardening behaviour with large tensile elongation as the initially annealed one.

K e y w o r d s: aluminium alloy, equal-channel angular pressing (ECAP), ultrafine grained microstructure, mechanical properties, recrystallization, grain growth

## 1. Introduction

The ECAP deformation technique has been widely used for the producing of ultrafine grained structure and mechanical properties improvement of AlMgSi alloys [1–10]. Authors of these works have achieved by suitable combinations of the heat treatment regimes (solution annealing, artificial ageing) and the ECAP processing a significant enhancement in strength, due to the solid solution grain refinement (down to grain size ∼ 150 nm), the rising of its dislocation density and the precipitation of $\beta''$- and/or $\beta'$-phase nanoparticles.

A very important requirement of the ultrafine grained AlMgSi alloys is the thermal stability of their structure and mechanical properties. Stability of the dislocation substructure within the solid solution ultrafine grains and thereby the strength of these alloys as well is ensured up to a temperature of ∼ 150 °C [9–11]. However, the ultrafine solid solution grains of these alloys are assumed to be stable against spontaneous extensive growth up to the critical temperature, which is about 250 °C [10]. An exposure of the severely deformed alloys at the higher temperature than the critical one caused the total alloy strengthening loss and the heterogeneous solid solution grains growth due to its discontinuous recrystallization [12, 13].

The aim of this paper is to analyze the influence

*Corresponding author: tel.: +421 55 602 2770; fax: +421 55 602 2243; e-mail address: martin.fujda@tuke.sk

Table 1. Chemical composition (wt.%) of the analyzed EN AW 6082 aluminium alloy

| Mg | Si | Mn | Fe | Zn | Cu | Al |
|---|---|---|---|---|---|---|
| 0.60 | 1.0 | 0.49 | 0.21 | 0.02 | 0.06 | bal. |

of severe plastic deformation realized by the ECAP process and subsequent post-ECAP annealing on the microstructure stability and mechanical properties of EN AW 6082 aluminium alloy.

## 2. Material and experimental procedure

An experimental program was carried out on the industrially extruded rods of EN AW 6082 aluminium alloy subjected to artificial ageing (T5 temper). The chemical composition of analyzed alloy is presented in Table 1. Prior to deformation in an ECAP die, the rods were annealed at 400 ℃ (holding time 2.5 h) and subsequently slowly cooled (cooling rate: 100 ℃ $h^{-1}$) to the room temperature in order to obtain the equilibrium solid solution with uniform distribution of relatively coarse particles of $Mg_2Si$- and Si-phase. The initially annealed alloy specimens with minimized effect of the precipitation strengthening were subjected to deformation in an ECAP die having a channels intersection angle $\Phi = 90°$ and an arc of curvature $\Psi = 37°$, up to 6 passes. ECA-pressing of specimens of size ø 10 mm × 100 mm was realized at room temperature following route $B_C$. After severe plastic deformation, the ECAPed specimens were subjected to post-ECAP annealing for 1 h in the temperature range 100–350 ℃ followed by cooling in air to room temperature.

Microstructure of the investigated alloy after the initial annealing, deformation in the ECAP die and after the post-ECAP annealing treatment was analyzed in the central zone of the specimen's cross-section using a light microscopy and a transmission electron microscopy (TEM) of thin foils. Microstructure of initially annealed alloy for light microscopy analysis was prepared by common metallographic grinding and polishing methods and finally revealed using Weck etchant. Thin foils for TEM observation were prepared using common metallographic methods and finally thinned in a solution of 25 % $HNO_3$ and 75 % $CH_3OH$ at the temperature of –30 ℃. TEM microstructure investigation was conducted at an accelerating voltage of 200 kV. The influence of the applied heat treatment, severe plastic deformation by ECAP process and the post-ECAP annealing on the mechanical properties of the analyzed alloy was evaluated by a tensile test. The tensile tests were carried out using short cylindrical samples ($d_0 = 5$ mm, $l_0 = 10$ mm) at the deformation rate of $2.5 \times 10^{-4}$ $s^{-1}$. Subsequently, the strength characteristics ($R_{p0.2}$ – yield strength and $R_m$ – tensile strength), uniform tensile elongation ($A_g$), tensile elongation ($A$) and reduction in area ($Z$) were determined.

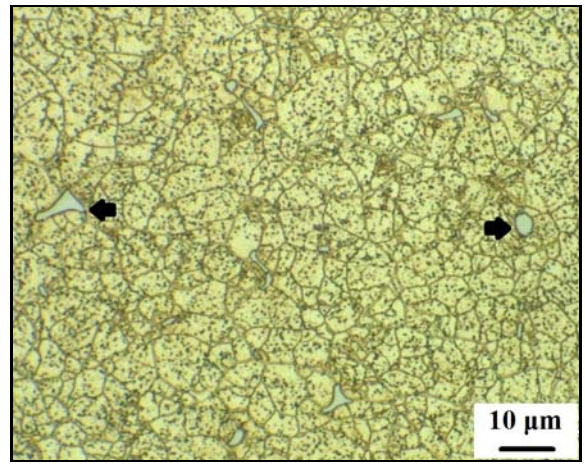


Fig. 1. Microstructure of the initially annealed EN AW 6082 alloy.

## 3. Results and discussion

### 3.1. Microstructure

All analyzed states of EN AW 6082 alloy contained intermetallic $\alpha$-$Al_8Fe_2Si$ phase particles of irregular morphology (Fig. 1 – marked by an arrow; mean particle size: 2.7 µm), the relatively coarse rod-like $Mg_2Si$- and Si-phase particles (Fig. 2; mean size of particles in initially annealed alloy state: 0.7 µm) and as well as fine dispersive Mn-rich particles (Fig. 2; mean particle size: 140 nm). The observed particles of all phases have been relatively uniformly distributed in the solid solution grains of the analyzed alloy states.

Figure 1 shows the equiaxed and fine grained (main grain size: 6.7 µm) $\alpha$-solid solution microstructure of the initially annealed alloy. Relatively low dislocation density and uniform distribution of dislocations in solid solution grains were detected by using TEM (Fig. 2). Severe plastic deformation of the initially annealed alloy state realized by ECAP deformation technique refined its microstructure considerably. It resulted in the formation of equiaxed ultrafine subgrains and/or grains (Fig. 3; main subgrain size: 370 nm), which contained a high density of dislocations. Refinement of the solid solution by application of the ECAP technique to similar size of subgrains (320–370 nm) was achieved also by authors [7–9] for the annealed condition of various AlMgSi alloys despite the fact that the initial solid solution grain size of the unde-

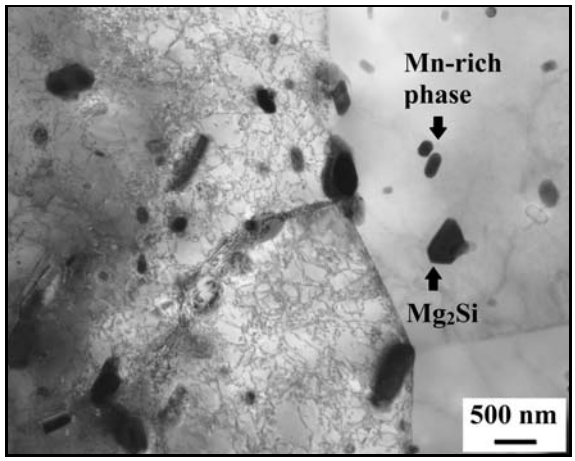


Fig. 2. TEM micrograph of the initially annealed EN AW 6082 alloy.

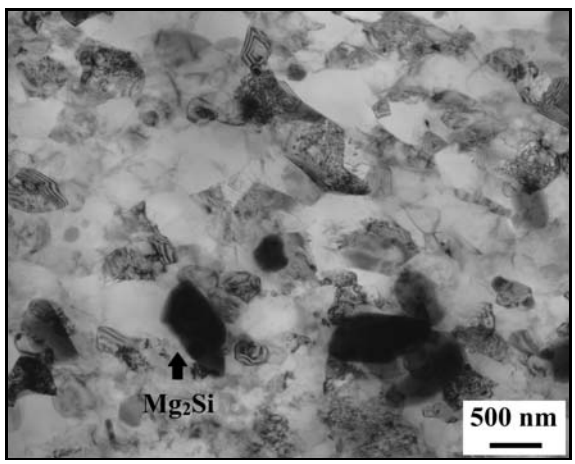


Fig. 3. TEM micrograph of the ECAPed EN AW 6082 alloy.

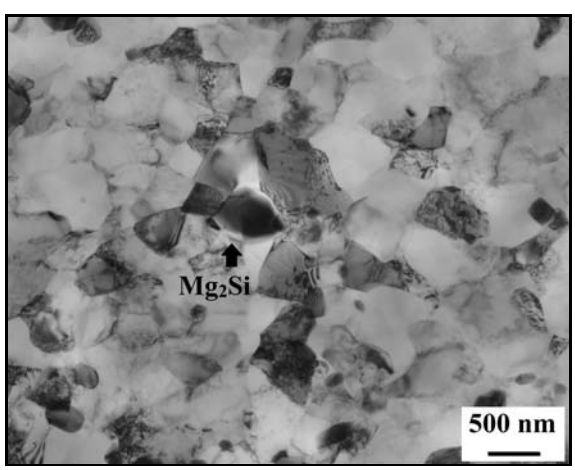


Fig. 4. TEM micrograph of the post-ECAP EN AW 6082 alloy annealed at 100 ℃.

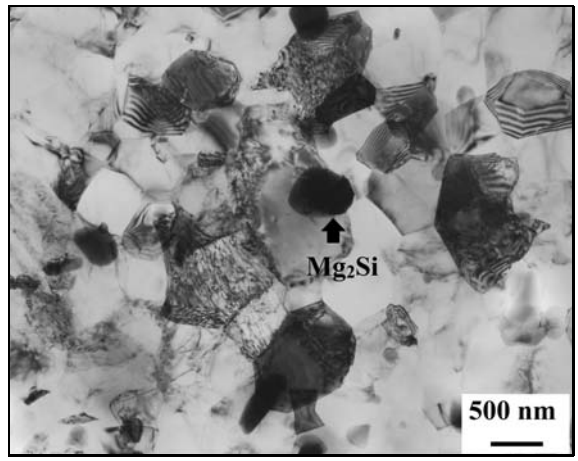


Fig. 5. TEM micrograph of the post-ECAP EN AW 6082 alloy annealed at 200 ℃.

formed alloys states was very different. The reason lies in the fact that the solid solution refinement efficiency of Al alloys obtained by the severe plastic deformation is dependent mainly on the alloying element contents in the deformed solid solution [14]. Since the contents of alloying elements (Mg and Si) in the solid solution are nearly the same in case of all AlMgSi alloys annealed states, the size of ultrafine grains formed by the repetitive ECA-pressing is also similar.

In order to analyze the thermal stability of the produced ultrafine grained alloy structure, the ECAPed samples were exposed to post-ECAP annealing at various temperatures ranging from 100 ℃ to 350 ℃. The post-ECAP annealing at the lowest temperature of 100 ℃ caused only a minor change in the size and morphology of ultrafine subgrains, which are shown in Fig. 4. Only a negligible subgrains growth to a size of 390 nm occurred. However, when ECAPed alloy was exposed to higher temperature of 200 ℃, the dislocation recovery and partial continuous recrystallization of the alloy ultrafine grain structure occurred (Fig. 5). The results were evident in a solid solution subgrains growth to a main size of 550 nm and a moderate dislocation density decrease. Figure 6 documents the continuously recrystallized ultrafine grain structure of the alloy which was formed during the post-ECAP annealing at 250 ℃. It is obvious that the solid solution subgrains and/or grains grew homogeneously up to size of 0.9 μm and the dislocation density within subgrains decreased markedly. After annealing at the highest temperature (350 ℃), a bimodal distribution of the grain size appeared (Fig. 7) due to the coexistence of coarse grains and fine grains. In the coarse solid solution grains (main grain size: 30 μm) a low dislocation density and curved boundaries were evident. Such coarse recrystallized grains are usually generated by coalescence of ultrafine subgrains with low-angle boundaries [15]. The fine equiaxed re-

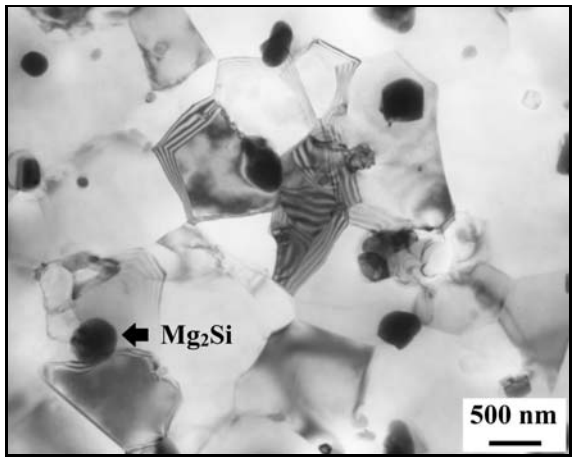


Fig. 6. TEM micrograph of the post-ECAP EN AW 6082 alloy annealed at 250 ℃.

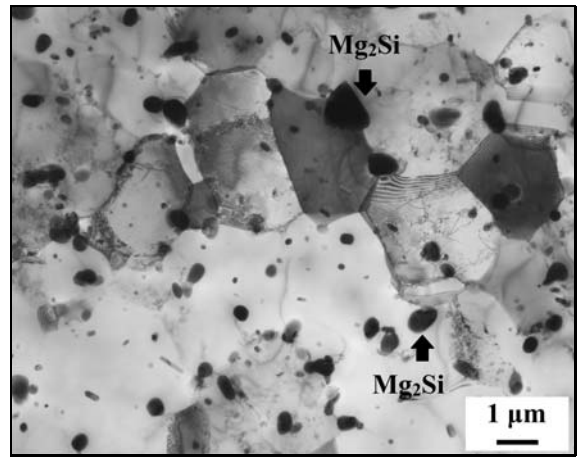


Fig. 7. TEM micrograph of the bimodal grain size microstructure of post-ECAP EN AW 6082 alloy annealed at 350 ℃.

crystallized grains (main grain size: 2.4 µm) having a low dislocation density were embedded in coarse grained ones, as it is shown in Fig. 7. The generation of a bimodal microstructure with grains of different sizes occurred in the strain-hardened aluminium alloys due to an uneven recrystallization process. This is a so-called discontinuous recrystallization, which occurred in severely deformed aluminium alloys with subgrains, mainly separated from each other by low-angle grain boundaries [12, 13]. An increase of the applied post-ECAP annealing temperature led to a partial dissolution of $Mg_2Si$ particles, which was followed with the new $Mg_2Si$-phase particles precipitation during alloy cooling down to room temperature in air. For this reason, the main size of $Mg_2Si$-phase particles (0.5 µm) measured after post-ECAP annealing at 350 ℃ was smaller than that for the initially annealed alloy state.

### *3.2. Mechanical properties*

The effect of severe plastic deformation realized by ECAP processing and post-ECAP annealing treatment on the tensile deformation behaviour and mechanical properties of the analyzed EN AW 6082 alloy is obvious from comparison of obtained mechanical properties (Table 2) and stress-strain curves (Fig. 8). Tensile strength ($R_m$) and, especially, yield strength ($R_{p0.2}$) of the initially annealed alloy state was significantly increased ($R_{p0.2}$ from 67 MPa to 200 MPa) by the repetitive ECA-pressing. On the other side, the alloy tensile ductility ($A_g$, $A$, $Z$) was deteriorated due to high straining. The tensile deformation behaviour of the ECAPed alloy state is typical for the severely strain hardened (ECAPed) AlMgSi alloy [2, 4–6, 8], for which low values of the uniform tensile elongation ($A_g$) and a high $R_{p0.2}/R_m$ ratio have been often found out.

The change in the tensile deformation behaviour and in mechanical properties of an alloy (Table 2, Fig. 8) that was induced by the post-ECAP annealing indicates that the strength of the severely deformed alloy was almost consistent up to 200 ℃. A moderate alloy strength increase and a ductility decrease caused by the post-ECAP annealing in the temperature range 100–200 ℃ was probably the result of the

Table 2. Mechanical properties and solid solution subgrain or grain sizes ($d_s$) of the analyzed EN AW 6082 aluminium alloy states

| Alloy state | | $R_{p0.2}$ (MPa) | $R_m$ (MPa) | $A_g$ (%) | $A$ (%) | $Z$ (%) | $d_s$ (µm) |
|---|---|---|---|---|---|---|---|
| Initially annealed | | 67 | 113 | 15.3 | 43.4 | 80.6 | 6.7 |
| ECAPed | | 200 | 234 | 2.0 | 24.9 | 56.4 | 0.37 |
| Post-ECAP annealed | 100 ℃ | 236 | 248 | 1.1 | 20.1 | 50.3 | 0.39 |
| | 200 ℃ | 222 | 234 | 0.5 | 18.9 | 59.2 | 0.55 |
| | 250 ℃ | 135 ($R_{eH}$) | 128 | 7.6 | 35.1 | 73.0 | 0.9 |
| | 275 ℃ | 123 ($R_{eH}$) | 126 | 9.8 | 38.6 | 75.6 | 1.6 |
| | 350 ℃ | 79 | 121 | 18.8 | 44.0 | 66.4 | – |

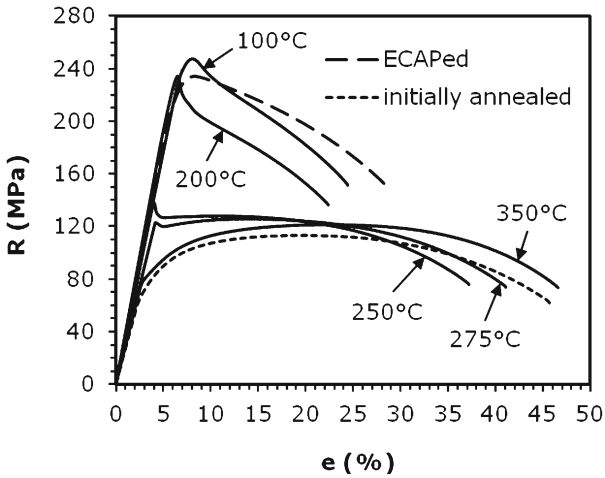


Fig. 8. Tensile stress-strain curves of initially annealed, ECAPed and post-ECAP annealed EN AW 6082 alloy.

coherent particle precipitation of the $\beta''$-phase from the deformed and slightly supersaturated solid solution. It is supposed that supersaturated solid solution was formed due to the deformation-induced dissolution of the former coarse $Mg_2Si$-phase, which occurred during ECAP-processing of the annealed and over-aged AlMgSi alloy states [7, 16]. Nevertheless, for a detailed identification of the particle precipitation an additional substructure analysis is required using the high-resolution transmission electron microscopy. The tensile test results obtained for the post-ECAP annealed alloys at temperatures of 250 ℃ and 275 ℃ (Table 2, Fig. 8) are in compliance with the observed changes of the alloy ultrafine grained structure. It can be seen (Table 2, Fig. 8) that tensile strength and yield strength decreased significantly after annealing of the severely deformed alloy at these temperatures. On the other side, the alloy stress-strain curves exhibited a narrow strain hardening region. Despite the fact, that the values of the tensile uniform elongation ($A_g$) and ductility ($A$, $Z$) of alloys in these states were only moderately lower than those for the initially annealed state, the yield strength ($R_{eH} = \sim 130$ MPa) of these annealed alloys was almost twice that of the initially annealed alloy (Table 2, Fig. 8). High grain boundary strengthening of these annealed alloys was provided by the very fine solid solution grains (grain size: 0.9–1.6 μm). Similar change for the mechanical properties and stress-strain curve shape, caused by the post-ECAP annealing of ultrafine grained aluminium alloys at identical temperatures has been observed in [12, 17]. With further increasing of the post-ECAP annealing temperature up to 350 ℃, the alloy yield strength decreased down to that of the initially annealed alloy. This fully discontinuously recrystallized alloy (at 350 ℃) exhibited the typical strain hardening behaviour with large tensile elongation (Fig. 8).

## 4. Summary and conclusions

Severe plastic deformation of annealed EN AW 6082 aluminium alloy realized by the ECAP process resulted in a considerable solid solution refinement. The equiaxed ultrafine subgrains (main subgrain size: 370 nm) with high dislocation density were formed. Refinement and strain hardening of alloy solid solution improved the alloy tensile strength while its tensile ductility was deteriorated.

The post-ECAP annealing of severely deformed alloy at temperatures lower than 200 ℃ did not significantly influence the ultrafine grained structure and mechanical properties of ECAPed alloy. A homogeneous solid solution grain size growth (up to 1.6 μm) occurred at higher annealing temperatures (up to 275 ℃) due to the continuous recrystallization of deformed solid solution grains. The yield strength of these annealed alloys with ultrafine or very fine grain size was almost twice that of the fine grained (grain size 6.7 μm) fully recrystallized initially annealed alloy. Fully discontinuously recrystallized alloy (at 350 ℃) with a bimodal grain size distribution exhibited typical strain hardening behaviour with low yield strength and large tensile elongation.

## Acknowledgements

This work was supported by the Scientific Grant Agency of the Slovak Republic as a grant project VEGA No. 1/0866/09.

## References

[1] Horita, Z., Fujinami, T., Nemoto, M., Langdon, T. G.: J. Mater. Process. Tech., *117*, 2001, p. 288. doi:10.1016/S0924-0136(01)00783-X
[2] Kim, W. J., Wang, J. Y.: Mater. Sci. Eng. A, *464*, 2007, p. 23. doi:10.1016/j.msea.2007.03.074
[3] Werenskiold, J. C., Roven, H. J.: Mater. Sci. Eng. A, *410–411*, 2005, p. 174. doi:10.1016/j.msea.2005.08.049
[4] Roven, H. J., Nesboe, H., Werenskiold, J. C., Seibert, T.: Mater. Sci. Eng. A, *410–411*, 2005, p. 426. doi:10.1016/j.msea.2005.08.112
[5] Dadbakhsh, S., Karimi Taheria, A., Smith, C. W.: Mater. Sci. Eng. A, *527*, 2010, p. 4758. doi:10.1016/j.msea.2010.04.017
[6] Hockauf, M., Meyer, L. W., Nickel, D., Alisch, G., Lampke, T., Wielage, B., Krüger, L.: J. Mater. Sci., *43*, 2008, p. 7409. doi:10.1007/s10853-008-2724-9
[7] Gutierrez-Urrutia, I., Munoz-Morris, M. A., Morris, D. G.: Mater. Sci. Eng. A, *394*, 2005, p. 399. doi:10.1016/j.msea.2004.11.025
[8] Fujda, M., Kvačkaj, T., Milkovič, O., Vojtko, M.: Materials Engineering, *15*, 2008, p. 14.
[9] McKenzie, P. W. J., Lapovok, R.: Acta Mater., *58*, 2010, p. 3198. doi:10.1016/j.actamat.2010.01.038

[10] Kashyap, B. P., Hodgson, P. D., Estrin, Y., Timokhina, I., Barnett, M. R., Sabirov, I.: Met. Mater. Trans. A, *40*, 2009, p. 3294. doi:10.1007/s11661-009-0036-6
[11] Kvačkaj, T., Fujda, M., Milkovič, O., Besterci, M.: High Temp. Mat. Pr.-Isr, *27*, 2008, p. 193. doi:10.1515/HTMP.2008.27.3.193
[12] Xing, Z. P., Kang, S. B., Kim, H. W.: J. Mater. Sci., *39*, 2004, p. 1259. doi:10.1023/B:JMSC.0000013884.69611.72
[13] Jazaeri, H., Humphreys, F. J.: Acta Mater., *52*, 2004, p. 3251. doi:10.1016/j.actamat.2004.03.031
[14] Iwahashi, Y., Horita, Z., Nemoto, M., Langdon, T. G.: Metall. Mater. Trans. A, *29*, 1998, p. 2503. doi:10.1007/s11661-998-0222-y
[15] Totten, G. E., Mackenzie, D. S. (Eds.): Handbook of Aluminum. Vol. 1. Physical Metallurgy and Processes. Boca Raton, Taylor & Francis/CRC Press 2003.
[16] Cabibbo, M., Evangelista, E., Vedani, M.: Metall. Mater. Trans. A, *36*, 2005, p. 1353. doi:10.1007/s11661-005-0226-9
[17] Horita, Z., Fujinami, T., Nemoto, M., Langdon, T. G.: Metall. Mater. Trans. A, *31*, 2000, p. 691. doi:10.1007/s11661-000-0011-8